Force Fields, Structures, and Properties of Poly(vinylidene fluoride) Crystals

Naoki Karasawa and William A. Goddard, III*

Materials and Molecular Simulation Center, Beckman Institute, 139-74, California Institute of Technology, Pasadena, California 91125

Received June 25, 1992; Revised Manuscript Received August 24, 1992

ABSTRACT: We report two new force fields for molecular dynamics simulations of poly(vinylidene fluoride), PVDF. The first, MSXX, was obtained with Hartree–Fock calculations of 1,1,1,3,3-pentafluorobutane plus experimental frequencies of the form I_p crystal. The second, the covalent shell model (MSXXS), was developed to also account for polarization. These force fields were used to predict structure and properties of nine stable structures of poly(vinylidene fluoride) crystals including the four experimentally observed forms plus a fifth crystal form suggested by Lovinger. In each case we used the force field to establish that the structure is mechanically stable and to predict cell parameters, elastic constants, dielectric constants, and piezoelectric constants.

I. Introduction

Poly(vinyldene fluoride) (PVDF) polymer (1) has piezoelectric and mechanical properties that make it technologically interesting. Thus, applying a voltage across a

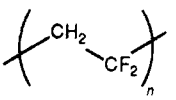

1

block of the material causes a strain, and applying a stress induces a voltage. In addition, PVDF exhibits four well-studied crystal forms (I–IV), with piezoelectric properties observed in two (I and IV). Thus, this material serves as a good test for molecular simulations since one must account for both the stability and nearly equal cohesive energies of several forms in addition to the mechanical and electrical properties.

In section II we develop two force fields (MSXX and MSXXS) for PVDF based on a combination of first principle quantum chemical (QC) calculations and experimental phonon frequencies of form I. Both force fields include the cross terms required for accurate vibrational (phonon) frequencies. MSXXS also includes the covalent shell model for describing polarizabilities. We do not readjust the force field (FF) parameters to fit observed crystalline properties (structure, elastic constants). Thus, the accuracy in predicting known properties can be used to assess the accuracy for prediction of unknown structures and properties.

These force fields are used to study the stabilities and properties of four observed forms of PVDF plus five additional forms which we find to be stable (including the antipolar form of III suggested by Lovinger[1]). The calculated properties include elastic constants (C_{ij}), piezoelectric moduli (d_{ij}), and the dielectric constant tensor (ϵ_{ij}).

II. Force Field

The force fields used in this paper are from first principle quantum mechanical calculations (although adjustments were made for the experimental frequencies of form I).

In developing the force fields for PVDF polymers, we first developed the MSXX force field for the 2,2-difluoropropane ($C_3H_6F_2$) molecule (where experimental frequencies are available) using ab initio Hartree–Fock (HF) calculations. We then modified this force field to fit the experimental structure and vibrational frequencies of the form I crystal. The torsional potentials are particularly important for PVDF since the various different crystalline forms have varying combinations of gauche and trans conformations. For this reason the torsional potential curves were obtained from accurate ab initio Hartree–Fock calculations for the 1,1,1,3,3-pentafluorobutane ($C_4H_5F_5$) molecule (2). In addition, the atomic charges were obtained from the Hartree–Fock calculations on 2 by fitting the long-range electrostatic field (potential-derived charges).

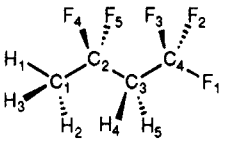

2

In order to account for changes in polarization due to applications of stress or electric fields, we modified the MSXX force field by including a *covalent shell model* (MSXXS) in which each atom is described in terms of two particles: the core (or nucleus) plus the shell (or effective valence electrons) as indicated in (1). The MSXXS

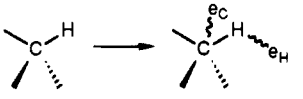

(1)

contains new parameters describing the atomic polarizability which we also determine from ab initio Hartree–Fock calculations.

We developed two independent sets of force field parameters for this polymer. The first set, MSXX, includes (i) valence interactions, such as the diagonal bond, angle, and torsion terms plus angle–stretch, stretch–stretch, one-center angle–angle, and two-center angle–angle cross terms; (ii) partial charges from HF wave functions of $C_4H_5F_5$ (2); and (iii) empirical van der Waals parameters. The second set, denoted MSXXS, includes all force field terms of MSXX plus the covalent shell model (CSM), but the valence parameters (i) and charges (ii) were modified to account for the CSM.

0024-9297/92/2225-7268$03.00/0

A. MSXX. Previously[2] we reported the MSXX force field for polyethylene derived from the Hessian biased force field (HBFF) from ab initio HF calculations of *n*-butane ($CH_3CH_2CH_2CH_3$). With HBFF, the errors in the predicted HF frequencies are corrected using experimental values, but the character (eigenfunctions) of the vibrational modes comes from theory. Assuming the valence parameters from *n*-butane apply to polyethylene, we calculated the structure, elastic constants, and vibrations of the polyethylene crystal. Here we found[2] excellent predictions for mechanical properties such as Young's modulus (within 3% of experiment) and phonon frequencies. To obtain all valence parameters needed for PVDF would require ab initio HF calculation on **3**. However,

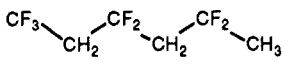

3

there are no experimental vibrational data for **3** to use in the HBFF, and indeed the only related molecule with sufficient experimental data is 2,2-difluoropropane (**4**). Consequently we instead obtained the HBFF for **4** and then corrected the parameters by readjusting to fit experimental frequencies of the form I crystal.[3]

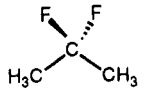

4

All quantum mechanical calculations were at the Hartree–Fock (HF) level using the 6-31G** basis set[4] (valence double ζ plus d polarization functions on C and F plus p polarization functions on H).

a. Charges. Partial atomic charges[5a] for the various atoms were obtained using the PS-Q program[5b] to calculate the (electrostatic) potential-derived charges (PDQ) for the Hartree–Fock wave function of the $C_4H_5F_5$ molecule (**2**). In this method, the charge density from the Hartree–Fock wave function is used to calculate the electrostatic potential at several thousand points outside the van der Waals (vdW) radii of the molecule and then atom-centered charges are optimized to fit this electrostatic potential function. In Table I we compare the charges from Mulliken populations and from charge equilibration (QEq) calculations[6] with the PDQ for both the trans and gauche forms of **2**. Here we see that the PDQ are very similar for the gauche and trans forms (rms difference of 0.015e). On the basis of these results, we selected the following charges (|e|, the charge of an electron) to be used for all calculations on PVDF:

$$Q_{CH} = -0.54 \quad Q_H = +0.18$$

$$Q_{CF} = +0.70 \quad Q_F = -0.26 \qquad (2)$$

(where CH and CF indicate the carbon bonded to H and F, respectively).

b. van der Waals Parameters. For carbon and hydrogen we used the van der Waals parameters previously determined from fitting lattice parameters, elastic constants, lattice phonons, and cohesive energies of the polyethylene crystal[2] and graphite crystal.[7] For the fluorine parameters, we use the parameters derived for CF_4 and poly(tetrafluoroethylene) crystals[8] (we could not find sufficient experimental data for fluorinated hydrocarbons). The accuracy in predicting the cell parameters of all four observed crystal forms of PVDF (vide infra) suggests that these vdW parameters are reasonably accurate.

Table I
Predicted Partial Charges for $C_4H_5F_5$ (2) from Various Calculations[a]

	trans (ϕ = 180°)			gauche (ϕ = 60°)[e]		
	PDQ[b]	QEq[c]	Mull[d]	PDQ[b]	QEq[c]	Mull[d]
			Charges			
C_1	−0.568	−0.185	−0.388	−0.561	−0.139	−0.396
H_1	0.175	0.212	0.160	0.161	0.204	0.151
H_2	0.160	0.128	0.136	0.170	0.192	0.155
H_3	0.160	0.128	0.136	0.159	0.137	0.132
C_2	0.733	0.663	0.781	0.730	0.650	0.789
F_4	−0.266	−0.475	−0.398	−0.268	−0.504	−0.399
F_5	−0.266	−0.475	−0.398	−0.264	−0.468	−0.392
C_3	−0.547	−0.012	−0.406	−0.586	−0.017	−0.429
H_4	0.182	0.092	0.171	0.201	0.183	0.188
H_5	0.182	0.092	0.171	0.191	0.105	0.173
C_4	0.717	1.193	1.119	0.729	1.097	1.102
F_1	−0.233	−0.498	−0.373	−0.229	−0.468	−0.369
F_2	−0.215	−0.431	−0.356	−0.220	−0.537	−0.357
F_3	−0.215	−0.431	−0.356	−0.214	−0.436	−0.349
			Group Charges			
$(CH_3)_1$	−0.073	+0.283	+0.044	−0.071	+0.394	+0.042
$(CF_2)_2$	+0.201	−0.287	−0.015	+0.198	−0.322	−0.002
$(CH_2)_3$	−0.183	+0.172	−0.064	−0.194	+0.271	−0.068
$(CF_3)_4$	+0.054	−0.167	+0.034	+0.066	−0.344	+0.027
			Dipole Moment (D)			
μ_x	−2.17 (−2.10)	−6.62	−3.22	−0.33 (−0.31)	−3.25	−0.29
μ_y	−3.17 (−3.02)	−7.21	−5.44	1.03 (0.98)	3.46	1.93
μ_z	0.0 (0.0)	0.0	0.0	−1.50 (−1.45)	−3.04	−2.36

[a] The charges used in simulations of PVDF are Q_{CH} = −0.54, Q_H = +0.18, Q_{CF} = +0.70, and Q_F = −0.26 for MSXX [see (2)] and Q_{CH} = −0.45, Q_H = +0.16, Q_{CF} = +0.77, and Q_F = −0.32 for MSXXS [see (15)]. These were based on the PDQ values of the trans form. The values of the dipole moment components calculated directly from the electron density are listed in parentheses under the PDQ value. [b] Potential-derived charges from PS-Q. [c] Charge equilibration, ref 6. [d] Mulliken populations. [e] Rigid rotation from ϕ = 180° to ϕ = 60°.

c. Torsional Potentials. Since we are interested in describing crystal forms with varying amounts of trans and gauche conformations, it is necessary to accurately describe the torsional potential of the chain, including both the trans and the gauche conformations. To do this, we used HF (6-31G** basis) to obtain the torsional potential curve for $C_4H_5F_5$ (**2**). In these calculations, the central C–C bond was rigidly rotated from the optimized structure at the trans geometry and the energy calculated at 30° increments (the energies are given in Table II). Using the charges and van der Waals parameters described above, we subtracted the electrostatic and van der Waals contributions to obtain the residual torsional potential. We also subtracted the torsional energy arising from F–C–C–H, F–C–C–C, and H–C–C–C terms, which were adjusted to fit experimental frequencies (see below). The Fourier transform $\{C_m\}$ of this residual torsional potential is given in Table III, along with an alternative form in terms of the potential barriers $\{V_m\}$ for each periodicity (this is the form used in Biograf/Polygraf). The simulations used the first six terms (m = 1, ..., 6) of this potential for the C–C–C–C torsional term. This fitted torsion curve is compared to the HF curve in Figure 1, where we see that it is accurate to about 0.05 kcal/mol.

d. Valence Parameters. With HBFF methodology[9b] we would optimize the force field for $C_4H_5F_5$ to obtain valence FF parameters. Since there are no experimental frequencies for $C_4H_5F_5$, we instead optimized the param-

Table II
Torsional Energy Curve for $C_4H_6F_6$ (2)[a]

		MSXX				MSXXS			
torsion angle	HF energy	vdW	Q^e	torsion[c]	C–C–C–C torsion[d]	vdW	$Q^{e,f}$	torsion[c]	C–C–C–C torsion[d]
0°, eclipsed	5.828	8.437	−2.198	−0.697	0.286	4.952	−3.098	−0.540	4.514
30°	3.061	4.873	−1.560	−0.763	0.511	2.874	−2.293	−0.649	3.129
60°, gauche	0.615	2.659	−1.093	−0.719	−0.232	1.404	−1.593	−0.652	1.456
90°	1.297	1.133	−0.847	−0.349	1.360	0.943	−1.251	−0.283	1.888
120°	2.784	1.524	−0.718	0.022	1.956	1.409	−0.983	0.091	2.267
150°	1.740	0.936	−0.286	0.067	1.023	0.833	−0.366	0.095	1.178
180°, trans	0.0	0.0	0.0	0.0	0.0	0.0	0.0	0.0	0.0
total[b]	−651.61444*h*	(3.851)	(−171.169)	(0.159)		(3.959)	(−201.073)	(0.301)	

[a] All energies are in kilocalories per mole unless otherwise noted. [b] Total energies of the trans form. [c] All torsion energies except for the C–C–C–C term. [d] Values used to fit C–C–C–C torsion. [e] Electrostatic. [f] Including shell polarization energies.

Table III
Fourier Transform of the Residual Torsion Potential for $C_4H_6F_6$

$$V(\phi) = \sum_{m=0}^{6} C_m \cos m\phi = V_0 + \sum_{m=1}^{6} (1/2)[|V_m| - V_m \cos m\phi]$$

	MSXX		MSXXS	
period (m)	C_m	V_m[a]	C_m	V_m[a]
0	0.7958	−1.1933	−2.0094	−4.6474
1	−0.4609	0.9218	1.2093	−2.4186
2	−0.4358	0.8715	0.2462	−0.4923
3	0.7622	−1.5244	1.0378	−2.0755
4	−0.0387	0.0775	0.0682	−0.1363
5	−0.1272	0.2543	0.0737	−0.1474
6	−0.1643	0.3287	−0.0029	0.0059

[a] In Table IV, these values are multiplied by 9 because the input to Biograf has each torsion term scaled by the number of torsion terms for each central bond.

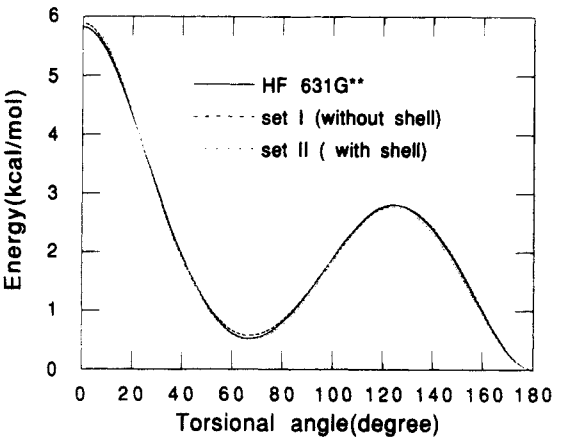

Figure 1. Torsional potential curves of $CH_3CF_2CH_2CF_3$ obtained by the Hartree–Fock calculations with the 631G** basis set and the molecular mechanics calculations (MSXX and MSXXS). The cis conformation has $\phi = 0°$.

eters to fit the vibrational frequencies of the form I crystal. In this fit we excluded the lattice modes since they are dominated by vdW and electrostatic terms which are not being readjusted. The valence terms used are the following.

(i) Morse bond stretch

$$E_b(R) = D_b[\chi^2 - 2\chi + 1]$$

$$\chi = e^{-\alpha(R-R_b)}$$

$$\alpha = (k_R/2D_b)^{1/2} \quad (3)$$

The bond distance (R_b) and force constant (k_R) are optimized, and the bond energy (D_b) is fixed (based on average bond energies). Here $E_b(R_b) = 0$.

(ii) cosine angle bend

$$E_a(\theta) = (1/2)C(\cos\theta - \cos\theta_a)^2$$

$$C = k_\theta/(\sin\theta_a)^2 \quad (4)$$

θ_a is the equilibrium angle, and k_θ is the force constant.

(iii) torsional potential

$$E_t(\phi) = \sum_m (1/2)[|V_m| - V_m \cos m\phi] \quad (5)$$

$m = 1, 2, ..., 6$ is used for the C–C–C–C torsional potential, and only $m = 3$ is used for other terms. For a given central bond jk, all possible $i \neq k$ bonded to j and $l \neq j$ bonded to k are included and normalized by the number of terms. Thus, for PVDF each C–C central pair leads to nine torsion terms (four FCCH, two FCCC, two CCCH, and one CCCC) which are added and normalized by dividing by 9.

(iv) angle–stretch cross terms

$$E_{ab} = D(\cos\theta - \cos\theta_e)(R - R_e)$$

$$D = -k_{R\theta}/(\sin\theta_e) \quad (6)$$

$k_{R\theta}$ is the force constant. If atoms i and k are bonded to j, we allow $D_{ij} \neq D_{kj}$.

(v) stretch–stretch cross terms

$$E_{bb} = k_{RR}(R - R_e)(\bar{R} - \bar{R}_e) \quad (7)$$

The bonds R and $\bar{R}$ share a common atom.

(vi) one-center angle–angle terms

$$E_{1aa} = G_{ij:kl}(\cos\theta - \cos\theta_e)(\cos\bar{\theta} - \cos\bar{\theta}_e)$$

$$G_{ij:kl} = \frac{k_{1\theta\theta}}{\sin\theta_e \sin\theta_e} \quad (8)$$

Equation 8 is used if atoms j, k, and l are all bonded to atom i. θ is (jik), and $\bar{\theta}$ is (jil). There are three such terms, all of which are included [$G_{ik:jl}$ and $G_{il:jk}$ in

Table IV
Force Field Parameters Used in the Calculations for PVDF[a]

		MSXX	MSXXS			MSXX	MSXXS
	van der Waals[c]				Torsion [See (5)]		
C	R_v	3.8837	3.8837	C–C–C–H	V_3	−4.4115	−4.4057
	ϵ_v	0.0844	0.0844	C–C–C–C	V_1	8.2966	−21.7670
	ζ_v	12.0	12.0	C–C–C–C	V_2	7.8439	−4.4309
H	R_v	3.1975	3.1975	C–C–C–C	V_3	−13.7195	−18.6795
	ϵ_v	0.016	0.016	C–C–C–C	V_4	0.6973	−1.2270
	ζ_v	11.8	11.8	C–C–C–C	V_5	2.2890	−1.3265
F	R_v	3.5380	3.5380	C–C–C–C	V_6	2.9580	0.0531
	ϵ_v	0.0211	0.0211	F–C–C–H	V_3	−1.0690	−1.0936
	ζ_v	16.0	16.0	F–C–C–C	V_3	5.3835	5.2046
	Bond Stretch [See (3)]				Angle Cross Terms [See (6) and (7)]		
C–C	R_b	1.5242	1.5269	H–C–H	$D_{H\theta}$	−20.5879	−17.2328
	k_R	682.1823	665.4933		k_{RR}	5.3363	2.3686
	D_b	(101.2)	(101.2)	C–C–H	$D_{C\theta}$	−26.0949	−27.8737
C–H	R_b	1.0789	1.0820		$D_{H\theta}$	−22.0763	−15.3201
	k_R	729.3088	715.6092		k_{RR}	0.9924	0.9978
	D_b	(106.7)	(106.7)	C_F–C–C_F[b]	$D_{C\theta}$	−20.1366	−16.3585
C–F	R_b	1.3457	1.3394		k_{RR}	18.6314	17.9468
	k_R	832.0755	876.8641	C–C_F–C[b]	$D_{C\theta}$	−27.1200	−17.3844
	D_b	(108.0)	(108.0)		K_{RR}	12.0600	11.8674
				F–C–C	$D_{F\theta}$	−62.9535	−69.8823
					$D_{C\theta}$	−48.9831	−42.5101
					k_{RR}	111.1305	109.2529
				F–C–F	$D_{F\theta}$	−75.9852	−74.3431
					k_{RR}	145.3960	127.2188
	Shells [See (11)]				One-Center Angle–Angle Cross Terms [See (8)]		
C	k_s	–	525.8132	$G_{CC:HC}$		2.4693	2.2899
H	k_s	–	2033.3751	$G_{CC:HH}$		−1.6436	−1.5733
F	k_s	–	811.5098	$G_{CH:CC}$		20.7375	18.6381
				$G_{CH:CH}$		0.8571	0.8027
				$G_{CC:FC}$		2.4667	2.4677
				$G_{CC:FF}$		27.3593	25.4020
				$G_{CF:CC}$		2.5382	2.6365
				$G_{CF:CF}$		−5.8372	−5.7643
	Angle Bend [See (4)]				Two-Center Angle–Angle Cross Terms [See (9)]		
H–C–H	k_θ	52.7607	55.8315	$F_{C:CC:H}$		28.5400	18.2612
	θ_a	116.4161	115.5015	$F_{C:CC:C}$		−10.6192	−9.6901
C–C–H	k_θ	64.7621	62.7458	$F_{F:CC:H}$		0.2414	0.2430
	θ_a	116.0913	116.5150	$F_{F:CC:C}$		29.2978	25.0190
C_F–C–C_F[b]	k_θ	178.4806	137.3946				
	θ_a	116.3318	119.6434				
C–C_F–C[b]	k_θ	155.5421	138.6187				
	θ_a	119.3277	119.7954				
F–C–C	k_θ	139.2072	136.0475				
	θ_a	114.8591	116.6151				
F–C–F	k_θ	184.7170	178.9011				
	θ_a	109.5665	111.3060				

[a] Units: kcal/mol, energy; Å, length; deg, angle; rad, angular force constant. van der Waals parameters and values in parentheses were not optimized. [b] C_F is used to specify the carbon in the CF_2 group to distinguish two kinds of C–C–C terms. [c] $E_{vdWIJ} = \epsilon_v\{A \exp[\zeta_v(1-\rho)] - B\rho^{-6}\}$ where $\rho = R/R_v$, $A = 6/(\zeta_v - 6)$, and $B = \zeta_v/(\zeta_v - 6)$.

addition to (8)].

(vii) two-center angle–angle terms

$$E_{2aa} = F_{i:jk:l}(\cos\phi)(\cos\theta - \cos\theta_e)(\cos\bar{\theta} - \cos\bar{\theta}_e)$$

$$F_{i:jk:l} = k_{2\theta\theta}/(\sin\theta_e \sin\bar{\theta}_e) \quad (9)$$

Equation 9 is used if atom i is bonded to j, j is bonded to k, and k is bonded to l. θ is (ijk), $\bar{\theta}$ is (jkl), and ϕ is the torsional angle of ij and kl about bond jk. As with torsions all i and l for a given jk are included.

The van der Waals parameters and charges were fixed during optimization of the valence parameters. The FFOPT program[9] [utilizing the singular value decomposition (SVD) methodology] was used to optimize the phonon frequencies while retaining zero stress and zero forces (ensuring that the structure remains optimum). The final force field parameters are shown in Table IV.

e. Results. The observed phonon frequencies (IR, Raman, Γ point) are given in Table V where we find an rms error of 17.2 cm^{-1}. In this table, vibrational frequencies of form II and form III crystals are also shown and these are compared with experiments. The agreement between theory and experiment for form II and form III is not as good as that of form I due to the presence of gauche conformations which are not fitted in the optimization procedures.

B. MSXXS: The Covalent Shell Model (CSM). In molecular dynamics simulations of organic molecules and polymers, the atomic charges representing the electrostatic properties of the molecule are usually fixed. But such fixed charges cannot describe the polarizability of a molecule since most of the polarizability effects come from the displacement of electronic clouds. Such polarization effects are expected to be important for the vibrational modes and even more important for the piezoelectric properties. Consequently we have extended the shell model (which has successfully accounted for polarization effects in ionic crystals[10]) for use in covalent molecules. In the shell model, each atom is represented by two charged points (shell and core) connected by an isotropic

Table V

(A) Vibrational Frequencies (cm^{-1}) of Intramolecular Modes for PVDF Crystals Using the MSXX and MSXXS Force Fields

(a) Form I_p

symmetry	MSXX	MSXXS	exptl[a]	symmetry	MSXX	MSXXS	exptl[a]
A_1	2983	2976	2980	B_1	1397	1399	1398
A_1	1429	1426	1428	B_1	1072	1075	1071
A_1	1276	1273	1273	B_1	480	473	468
A_1	887	882	840	B_2	3017	3020	3022
A_1	511	508	508	B_2	1165	1164	1177
A_2	980	980	980	B_2	841	843	880
A_2	267	267	260	B_2	447	449	442
rms error	17.2	15.7		[d]			

(b) Form II_{ad}

symmetry	MSXX	MSXXS	exptl[b]	symmetry	MSXX	MSXXS	exptl[b]
A_g	3034	3038	2990	B_g	3032	3036	3030
A_g	2991	2976	2970	B_g	2992	2978	2980
A_g	1382	1390	1430	B_g	1418	1415	1442
A_g	1351	1353	1406	B_g	1302	1304	1384
A_g	1219	1208	1296	B_g	1208	1210	1200
A_g	1182	1200	1150	B_g	1145	1144	1190
A_g	1091	1078	1058	B_g	1129	1137	1064
A_g	1010	1009	976	B_g	1011	1010	940
A_g	849	851	876	B_g	934	929	885
A_g	844	830	841	B_g	881	865	800
A_g	632	626	612	B_g	723	714	766
A_g	510	503	488	B_g	533	531	536
A_g	436	428	414	B_g	417	412	
A_g	295	292	287	B_g	368	372	357
A_g	260	250	206	B_g	281	275	216
A_g	108	105	75	B_g	207	205	176
A_u	3031	3036	3017	B_u	3035	3039	3017
A_u	2989	2977	2977	B_u	2992	2976	2977
A_u	1400	1402	1383	B_u	1380	1389	1420
A_u	1290	1289		B_u	1351	1353	1399
A_u	1205	1208	1209	B_u	1218	1208	1290
A_u	1143	1143	1182	B_u	1180	1198	1149
A_u	1128	1136		B_u	1092	1079	1056
A_u	1010	1011	1067	B_u	1010	1009	976
A_u	934	929	878	B_u	849	850	873
A_u	879	865	795	B_u	842	829	853
A_u	725	715	766	B_u	632	626	612
A_u	529	527	531	B_u	509	503	489
A_u	419	415	389	B_u	433	426	410
A_u	367	370	355	B_u	298	294	288
A_u	279	273	215	B_u	267	259	208
A_u	208	206	176	B_u	107	104	100
rms error	39.4	38.5					

(c) Form III_{pu}

symmetry	MSXX	MSXXS	exptl[c]	symmetry	MSXX	MSXXS	exptl[c]
A'	3022	3028	3032	A''	3021	3025	3032
A'	3015	3019	3022	A''	3015	3022	3022
A'	2984	2977	2990	A''	2984	2974	2990
A'	2976	2967	2985	A''	2976	2964	2985
A'	1411	1414	1400	A''	1420	1419	1427
A'	1391	1400	1385	A''	1383	1393	1385
A'	1379	1381	1365	A''	1359	1363	1365
A'	1250	1246	1320	A''	1319	1322	1330
A'	1233	1238	1250	A''	1251	1247	1274
A'	1194	1203	1234	A''	1185	1192	1205
A'	1164	1166	1190	A''	1170	1180	
A'	1157	1156	1175	A''	1159	1163	1134
A'	1147	1150		A''	1101	1103	1115
A'	1097	1089	1075	A''	1093	1084	1052
A'	1005	1005		A''	1011	1009	
A'	978	977	964	A''	991	987	
A'	947	935	874	A''	896	892	878
A'	891	879	858	A''	864	859	842
A'	869	862	835	A''	857	852	791
A'	843	843	811	A''	854	842	748
A'	737	725	776	A''	700	694	723
A'	553	547	614	A''	618	610	656
A'	548	544	539	A''	534	530	512
A'	507	502	484	A''	511	508	500
A'	448	447	442	A''	454	450	432
A'	411	408		A''	437	439	404

Table V (Continued)

(c) Form III_{pu}

symmetry	MSXX	MSXXS	exptl[c]	symmetry	MSXX	MSXXS	exptl[c]
A'	375	379	370	A''	345	345	350
A'	333	324	299	A''	313	313	304
A'	274	273	286	A''	277	270	267
A'	226	222		A''	265	255	
A'	185	181	172	A''	246	240	
A'	135	130	130	A''	160	157	172
A'	102	102	98	A''	135	133	
A'	65	63	84	A''	65	64	
rms error	29.7	27.3					

(B) Vibrational Frequencies (cm^{-1}) of Lattice and Twist Modes of PVDF Crystals Using the MSXX and MSXXS Force Fields[e]

form	type	symmetry	MSXX	MSXXS	exptl[b]	form	type	symmetry	MSXX	MSXXS	exptl[b]
I_p	R_0	B_2	87	88	–	III_{pu}	T_a	A'	52	50	
II_{ad}	T_a	A_g	43	40	52		T_c	A'	23	25	
	T_c	A_g	23	30	29		R_π	A''	62	62	
	R_π	A_u	66	68	53		T_b	A''	54	52	
	R_0	B_g	73	71	99		R_0	A''	42	40	
	T_b	B_g	62	60	–						

[a] Reference 3. [b] Reference 35. [c] Reference 36. [d] The two sets of intermolecular modes are split by 0–2 cm^{-1}. We show the lower one for each case. [e] Here T_i indicates a translational mode in the i lattice direction, and R_j indicates a librational (twist) mode where $j = 0$ indicates that the molecules within the unit cell have the same phase and $j = \pi$ indicates that the molecules have the opposite phase.

harmonic spring:

$$\delta E = (1/2)k_s(\delta R)^2 \tag{10}$$

where δR is the distance between the shell and core. Equation 10 leads to an atomic or shell polarizability of

$$\alpha_s = C_{unit}Z^2/k_s \tag{11a}$$

$$k_s = C_{unit}Z/\alpha_s \tag{11b}$$

where Z is the shell charge ($|e|$) and $C_{unit} = 332.0637$ converts units so that energy is in kilocalories per mole while distance is in angstroms (leading to α_s in cubic angstroms).

a. Nonbond Exclusions. Defining the total charge (shell plus core) on an atom i as Q_i, then the total charges on the shell and core are

$$q_{is} = -Z_i$$

$$q_{ic} = Q_i + Z_i \tag{12}$$

A complication of using the shell model for covalent systems is that standard force fields generally exclude the Coulomb interactions between two bonded atoms (1–2 interactions) and between two atoms bonded to a common atom (1–3 interactions). In addition they sometimes ignore or scale the 1–4 interactions. In order to retain the possibility of such exclusions while using the shell model, we use the following conventions: (1) If 1–2 interactions are excluded (assumed so for PVDF), then we exclude Q_1Q_2, Z_1Q_2, and Q_1Z_2 terms from the electrostatic interactions while including Z_1Z_2 terms. (2) If 1–3 interactions are excluded (we assume so for PVDF), then we exclude Q_1Q_3, Z_1Q_3, and Q_1Z_3 terms while including Z_1Z_3 terms. (3) If 1–4 interactions are excluded or scaled (for PVDF full 1–4 interactions were used), then we apply the scaling to all Q_1Q_4 terms while including all Z_1Z_4, Z_1Q_4, and Q_1Z_4 terms at full value.

Thus, all dipole interactions from shell polarizations are included while 1–2 and 1–3 exclusions are dealt with in the normal fashion.[11] We find that this convention leads to similar valence parameters for the MSXX and MSXXS force fields.

The vdW parameters of the shells were taken as zero, so that the core atoms carry all vdW interactions.

b. Molecular Polarizability. The molecular polarizability, α, is determined by including all dipole–dipole interactions of atomic polarizability centers and is given by[12]

$$\alpha_{a,b} = C_{unit}\sum_{ij} q_i q_j D_{ia,jb} \tag{13a}$$

where the sum is over all charged centers (shells and cores) and $D_{ia,jb}$ is the inverse of the second-derivative matrix (Hessian), $\Phi_{ia,jb}$

$$D_{ia,jb} = \Phi^{-1}_{ia,jb} \qquad \Phi_{ia,jb} = \frac{\partial^2 V}{\partial r_{ia}\,\partial r_{jb}} \tag{13b}$$

after eliminating translational and rotational components. Here, V is the total potential energy of the system and r_{ia} is the a component ($a = x$, y, or z) of the position vector for center i. With no net atomic charges ($Q_i = 0$) this model gives the same molecular polarizability as the atom–dipole interaction model of Applequist.[13] The CSM is easily incorporated in molecular-mechanics calculations since the shells are treated as additional ions so that no special treatment is necessary for energy minimization or calculation of mechanical properties. In vibrational frequency calculations, we assign the shells to have the mass of an order of a free electron (0.001 in atomic mass units, $^{12}C = 12.000$). Core (real) vibrational frequencies are not sensitive to shell mass if it is less than $\simeq 1/100$ of the hydrogen mass. Thus, the first $3N - 6$ (or $3N - 3$ for a crystal) vibrational modes (where N is the number of atoms) correspond to the real vibrations (the others lead to collective or plasmon modes for the shell electrons).

c. Calculation of the Shell Parameters. The shell polarizabilities, α_i, for hydrogen, carbon, and fluorine were determined from Hartree–Fock calculations.[4] We calculated polarizabilities of fluoromethane (CFH_3) and found that HF calculations using a basis set with extra polarization functions (DZ95(3d,2p)) gave reasonably good polarizabilities.[12] For 2,2-difluoropropane (4) we obtained the polarizability tensors in Table VI. Using the results for the DZ(3d,2p) basis and assuming shell charges of $Z = 1$ on all atoms, we find optimum shell polarizabilities of

$$\alpha_C = 0.632\ Å^3 \qquad \alpha_F = 0.409\ Å^3$$

$$\alpha_H = 0.163\ Å^3 \tag{14}$$

which describe the molecular polarizability to within about

Table VI
Molecular Polarizability (Å³) of 2,2-Difluoropropane (4)[a]

basis set[b]	α_{11}	α_{22}	α_{33}	rms error
DZ95**	4.63	5.01	4.71	0.67
DZ95(3d,2p)	5.30	5.98	5.45	0
MSXXS[c]	5.33	5.64	5.39	0.20
charges only	0.50	0.57	0.60	4.89

[a] The experimental geometry (geometry from ref 37) was used (all carbon atoms are in the yz plane, and the z axis is the C_2 axis). [b] DZ95** is a standard basis set with valence double ζ plus polarization functions (ref 4). In DZ95(3d,2p), extra polarization functions are added (2d for C and F, 1p for H) and their exponents are taken as the same as those of valence atomic basis functions. [c] Shell polarizabilities [shown in (14)] were fitted to reproduce DZ95(3d,2p) results.

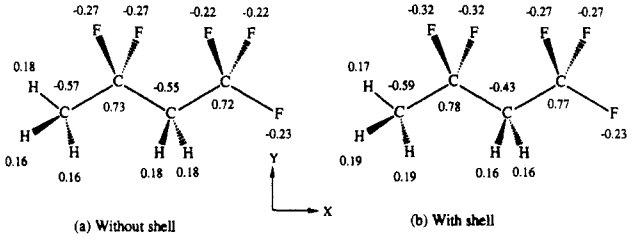

Dipole Moment (Debye)

	HF	Without Shell	With Shell
P_x	-2.10	-2.17	-2.19
P_y	-3.07	-3.17	-3.13
P_z	0	0	0

Figure 2. Net atomic charges (in units of electron charge) obtained by fitting the electrostatic potential from the Hartree–Fock calculations of $C_4H_5F_5$ with and without shell parameters. Calculated dipole moments are also shown.

6%. Without the shell terms the polarizability components are about 90% too small.

d. Reoptimization of Charges. With CSM, the center of each shell is displaced from the core, leading to atomic dipoles (and higher order multipoles) at each center. As a result the net charges Q_i on each atom were reoptimized to fit the electrostatic fields from the HF calculations. This was done iteratively since the displacement of the shell is dependent on the charges of the other centers. We started with the net atomic charges of MSXX, and the shell positions were optimized (with Polygraf) using fixed core positions. Then PS-Q was used to subtract the electrostatic potential arising from the induced dipoles from the total Hartree–Fock potential and then to fit new atomic charges (Q_i) to this residual electrostatic potential. These charges were in turn used to obtain new shell positions (Polygraf), etc. For $C_4H_5F_5$ we found three iterations to be sufficient for determining the charges to better than 0.01e. Figure 2 shows the net atomic charges of $C_4H_5F_5$ before and after the fitting. Dipole moments from HF and PS-Q are also shown. With or without CSM, agreement between HF and PS-Q is good. From these results we assigned the charges as

$$Q_{CH} = -0.45 \quad Q_H = 0.16$$

$$Q_{CF} = 0.77 \quad Q_F = -0.32 \qquad (15)$$

for all MSXXS calculations on PVDF.

e. van der Waals Parameters. For MSXXS we take the van der Waals parameters to be the same as in MSXX with no vdW interactions involving the shells.

f. Torsion Parameters. Since the electrostatic interactions are different for MSXX and MSXXS, we recalculated the electrostatic energy for $C_4H_5F_5$ using CSM (see Table II) (allowing optimized shell positions for each conformation). These results were used to determine a new torsional potential curve (Table II) and new Fourier components (Table III). The final fit is shown in Figure 1.

g. Valence Parameters. We started with the valence parameters for MSXX and reoptimized them to include the changes arising from the shell model. The final force field parameters are shown in Table IV. We find that including polarization effects in the force field leads to smaller valence spring constants. This in turn leads to smaller elastic constants (vide infra).

h. Results. The vibrational frequencies are shown in Table V. For MSXXS, the rms difference between calculated and experimental values for form I is 15.7 cm^{-1}.

i. Other Approaches. Previous approaches to accounting for atomic polarizability involved using polarizable centers. Thus, Applequist[13] developed an atom–dipole interaction model to calculate the optical properties of the molecules, and Boyd and Kesner[14] introduced a polarization-mutual induction model to represent inductive effects of the molecules. These approaches lead to errors of 2.2% and 5.8% for describing average polarizabilities of halomethane molecules, about the same as CSM.

III. Crystal Calculations

Table VII summarizes various characteristics of the four observed structures of PVDF plus the five other stable structures that we studied. All nine of these structures are stable (positive definite elastic constant tensor and all phonon frequencies positive). The three common notations for the four observed structures are {I,II,III,IV}, {$\beta,\alpha,\delta,\gamma$}, or {I,II,III,II$_p$}. In order to simplify reference to all 10 forms, we believe that the best notation would be T, TG, and T_3G (in place of I, II, and III) to indicate the conformation of the chain, followed by subscripts p and a to indicate *parallel* or *antiparallel* orientation of the chains (about the chain axis), followed by subscripts u and d to indicate *up–up* or *up–down* relative directions of adjacent chains. A less severe change from current notation (and the one we will use in this paper) is to use I, II, and III to indicate conformation [T, TG, and T_3G] followed by the same subscripts. Thus, for the four observed structures, I becomes I_p (or T_p), II becomes II_{ad} (or TG_{ad}), III becomes III_{pu} (or T_3G_{pu}), and IV becomes II_{pd} (or TG_{pd}). Form II normally has a statistical distribution of up–up and up–down, so that II becomes II_a while IV becomes II_p. All nine forms are shown in Figure 3, and the structural parameters (calculated and observed) are in Table VIII. We did not calculate the antipolar form, I_a, of the all-trans form, I_p.

Observations about the four experimentally characterized crystal forms of PVDF are as follows.

Form I (β form) has a planar-zigzag type of conformation (all trans), with two chains in the unit cell.[15] These chains are aligned in the direction parallel to the b axis, leading to a polar crystal (piezoelectricity). For this case up–up and up–down are the same so that it is denoted as I_p (or T_p).

Form II (α form) has the TGT$\bar{G}$ molecular conformation with two chains in the unit cell. These chains are aligned antiparallel (nonpolar) in a direction perpendicular to the chains. The experimental structure is interpreted[16] in terms of a statistical average over the up–up and up–down orientations. Thus, we use II_a (or TG_a) to denote the statistically averaged case and II_{au} and II_{ad} (TG_{au} and TG_{ad}) for the two separate orientations.

Table VII
Names and Characteristics for Various Forms of Crystalline Poly(vinylidene fluoride), PVDF

name										
new simple	I_p	I_a	II_{pu}	II_{pd}	II_{au}	II_{ad}	III_{pu}	III_{pd}	III_{au}	III_{ad}
new complete	T_p	T_a	TG_{pu}	TG_{pd}	TG_{au}	TG_{ad}	T_3G_{pu}	T_3G_{pd}	T_3G_{au}	T_3G_{ad}
Roman	I		(IV)	IV	(II)	II	III		V	
Roman′	I		(II_p)	II_p	(II)	II	III_p		III_a	
Greek	β		(δ)	δ	(α)	α	γ			
conformation	T	T	TGTḠ	TGTḠ	TGTḠ	TGTḠ	$T_3GT_3Ḡ$	$T_3GT_3Ḡ$	$T_3GT_3Ḡ$	$T_3GT_3Ḡ$
alignment										
∥ chain			u–u	u–d	u–u	u–d	u–u	u–d	u–u	u–d
⊥ chain	p	a	p	p	a	a	p	p	a	a
polar										
∥ chain	no	no	yes	no	yes	no	yes	no	yes	no
⊥ chain	yes	no	yes	yes	no	no	yes	yes	no	no
space group	C_{m2m}		C_c	$P2_1cn$	$Pca2_1$	$P2_1/c$	C_c	P_{na2_1}	$Pca2_1$	$P2_1/c$
	C_{2v}^{14}		C_s^4	C_{2v}^9	C_{2v}^5	C_{2h}^5	C_s^4	C_{2v}^9	C_{2v}^5	C_{2h}^5
energy										
MSXX	0		0.68	0.69	0.85	0.78	0.30	1.90	0.46	1.20
MSXXS	0			0.67		0.72	0.46		0.64	
observed	yes		stat	stat	stat	stat	yes	no	no	no
piezoelectric	yes		yes	yes	yes	no	yes	yes	yes	no
$d_{\perp\perp}$[a] (MSXXS)	−18.8			−2.9		0	−2.7		0	
Young mod (E_c)										
MSXX	293			163		153	113		102	
MSXXS	277			150		141	107		92	
compress (β)										
MSXXS	15.2			13.6		13.6	14.7		13.5	

[a] Piezoelectric modulus connecting a change of polarization in the direction perpendicular to the chain with a tension stress in that direction.

Table VIII
Optimized Energy (kcal/mol per CH_2CF_2) and Cell Parameters (Å, deg) of Various Forms of PVDF with Parallel (Up–Up) and Antiparallel (Up–Down) Alignment of Chains in the Unit Cell[a]

	form I_p	form II_{ad} up–down	form II_{au} up–up	form III_{pu} up–up	form III_{pd} up–down	form II_{pd} up–down	form II_{pu} up–up	form III_{au} up–up	form III_{ad} up–down
space group	*Cm2m*	$P2_1/c$	$Pca2_1$	*Cc*	$Pna2_1$	$P2_1cn$	*Cc*	$Pca2_1$	$P2_1/c$
				MSXX					
energy	−121.67	−120.89	−120.82	−121.37	−119.77	−120.98	−120.99	−121.21	−120.47
a	8.61 (8.58)	5.07 (4.96)	5.09	5.02 (4.96)	5.24	5.08 (4.96)	5.20	9.68	6.04
b	4.72 (4.91)	9.47 (9.64)	9.50	9.53 (9.67)	9.27	9.32 (9.64)	9.36	4.98	9.01
c	2.56 (2.56)	4.59 (4.62)	4.59	9.14 (9.20)	9.28	4.58 (4.62)	4.58	9.13	9.26
α	90.0 (90.0)	90.1 (90.0)	90.0	90.0 (90.0)	90.0	90.1 (90.0)	90.0	90.0	90.0
β	90.0 (90.0)	92.0 (90.0)	90.0	97.7 (93.0)	90.0	90.0 (90.0)	104.0	90.0	120.0
γ	90.0 (90.0)	90.0 (90.0)	90.0	90.0 (90.0)	90.0	90.0 (90.0)	90.0	90.0	90.0
				MSXXS					
energy	−129.92	−129.00		−129.26		−129.05		−129.08	
a	8.55 (8.58)	5.05 (4.96)		4.98 (4.96)		5.05 (4.96)		9.65	
b	4.71 (4.91)	9.37 (9.64)		9.45 (9.67)		9.23 (9.64)		4.93	
c	2.56 (2.56)	4.58 (4.62)		9.13 (9.20)		4.58 (4.62)		9.12	
α	90.0 (90.0)	90.1 (90.0)		90.0 (90.0)		89.8 (90.0)		90.0	
β	90.0 (90.0)	92.2 (90.0)		96.8 (93.0)		89.9 (90.0)		90.0	
γ	90.0 (90.0)	90.0 (90.0)		90.0 (90.0)		90.0 (90.0)		90.0	

[a] In all forms, the *c* axis corresponds to the chain direction. Experimental cell parameters are shown in parentheses where available. For MSXXS, only observed structures are shown.

Form III (γ form) has a molecular conformation[1,17] of $T_3GT_3Ḡ$ with two chains packed in the unit cell. These chains are aligned parallel (polar) in the direction perpendicular to the chains. Thus, we denote this as III_{pu} (or T_3G_{pu}). The existence of an antipolar analogue III_{au} (or T_3G_{au}) of this form was suggested by Lovinger[1] (sometimes denoted V).

Form IV (δ or II_p form) has the same molecular conformation as form II, but the two chains of the cell are aligned in a polar fashion in a direction perpendicular to the chains.[18] The chains are observed to have a statistical up–down packing.[18] Thus, for the statistical case we denote this as II_p (or TG_p).

The MSXX and MSXXS force fields were first used to optimize[19] the atomic coordinates using the fixed experimental cell parameters for all forms. The energy, elastic constants, dielectric constants, and piezoelectric constants were then calculated from analytical second derivatives by using the formula derived by Born and Huang.[20] Then we allowed cell deformations and reoptimized the cell parameters and internal coordinates. In all the calculations (including parameter fitting), nonbond interactions were calculated using the ABCA method[21] (based on Ewald procedures), with an accuracy of 0.1 kcal/mol for both Coulomb and van der Waals terms.

IV. Energy and Cell Parameters

The energy and optimized cell parameters for the four experimental forms are shown in Table IX. Each single polymer chain for conformations II and III has net dipole components in both the chain direction and in a direction perpendicular to the chain. In the crystals, it is generally assumed that the experimental samples have statistically[16-18] disordered orientations of the dipoles along the chain direction. For our calculations, we used the perfectly aligned chains allowed by the space group symmetry (II_{ad}, II_{pd}, III_{pu}). Calculations assuming other chain alignments in the unit cell were also performed with the results in section VII.

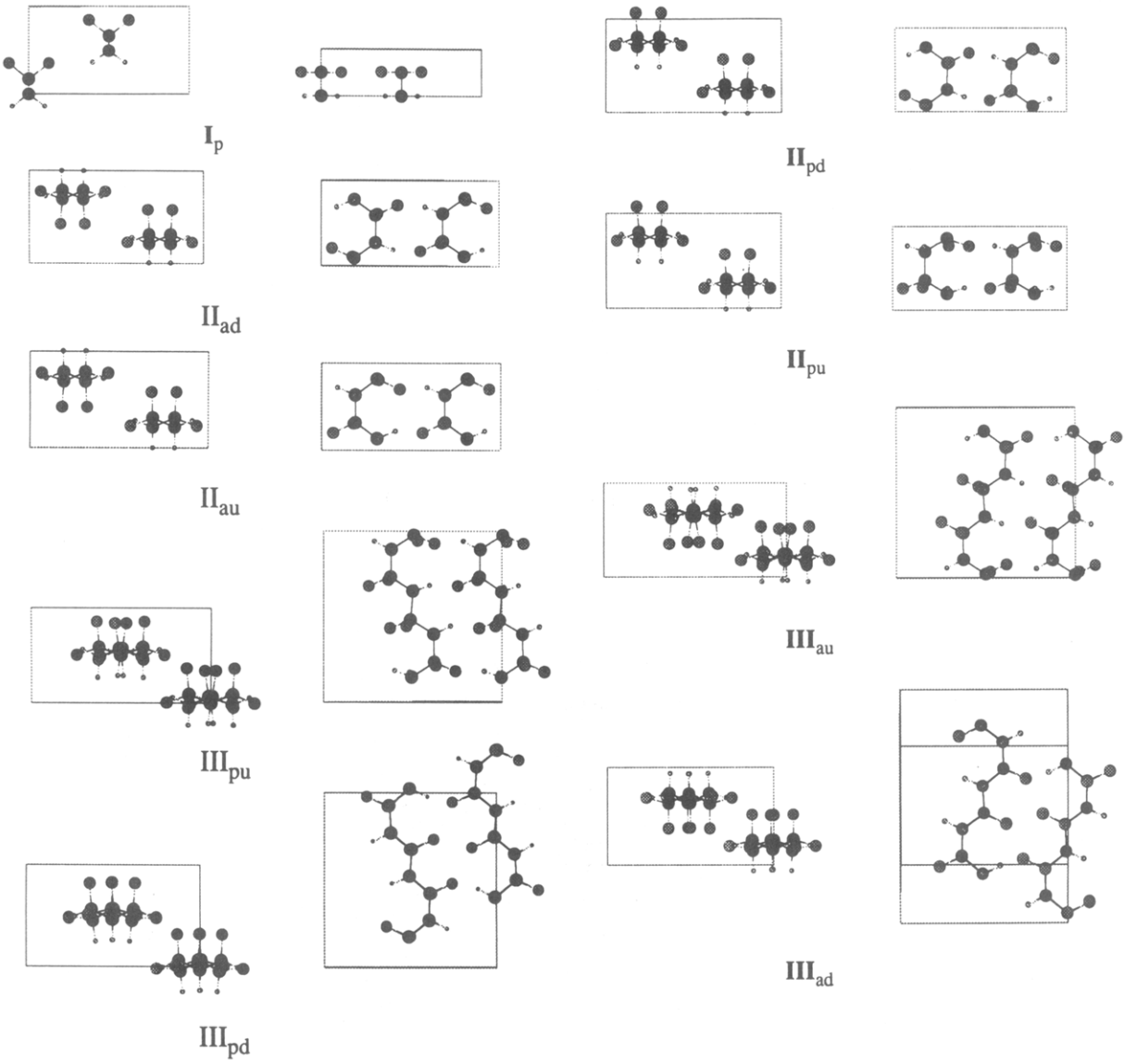

Figure 3. Crystal packing of the nine stable crystal forms for PVDF.

Table IX also includes the zero-point energies and free energies at 300 K (calculated by using the quasi harmonic approximation[20]) for these five forms. In these calculations, the (core) phonon frequencies are calculated at uniformly-spaced wave vectors in the Brillouin zone, and these are used to calculate zero-point energies and free energies utilizing the quantum partition functions for harmonic oscillators. The number of wave vectors used is 1000 (10 × 10 × 10) for MSXX and 125 (5 × 5 × 5) for MSXXS.

For both force fields, MSXX and MSXXS, we find that the differences in total energy and free energy at 300 K of these four forms are quite small (within 1 kcal/mol per monomer unit). This is encouraging because we would expect that experimentally observable forms should be within 1 kcal/mol. These results suggest that the vdW, Q, and torsional potentials are accurate. It is interesting that forms II_{ad} and II_{pd} have almost the same electrostatic energy although the chain alignment is different. The vdW energy seems to dominate the determination of which form is stable.

Optimized cell parameters are shown in Table VIII. The rms difference between the calculations and the experiment is 0.14 Å for cell lengths for MSXX and 0.17 Å for MSXXS. The cell angles are all 90° except for β in forms II_{ad} and III_{pu}. The differences between the calculations and the experiment of this angle are about 2° for form II_{ad} and about 4° for form III_{pu}. One reason for differences is that the calculations correspond to the values at 0 K, but the experiments were usually at room temperature.

V. New Crystal Form

Lovinger suggested[1] that an antipolar analogue (denoted III_{au} or V) of the form III_{pu} crystal might exist. We examined this possibility by optimizing the structure by starting with form III_{pu}, rotating one chain about the chain axis by 180° (to align these chains in the antipolar fashion), and then optimizing atom positions and cell parameters. The energy of this form is comparable to other forms (see Table IX).

The elastic-stiffness tensor (C_{ij}) shows that this is a stable form. These calculations support the stability of the Lovinger form. The cell is orthorhombic, and the space group is $Pca2_1$ (C_{2v}^5). Figure 4 shows the end view and the side view of the structure.

VI. Elastic, Dielectric, and Piezoelectric Properties

Elastic, dielectric, and piezoelectric properties were calculated for all forms using analytic second derivatives of energy at the optimized structures.[20] In particular, these calculations include long-range Coulomb interactions using

Table IX
Energies (kcal/mol) per CH_2CF_2 for All Forms of PVDF at Experimental (Exptl) and Optimized (Opt) Cell Parameters[a]

	form I_p		form II_{ad}		form III_{pu}		form II_{pd}		form III_{au}	
	exptl	opt	exptl	opt	exptl	opt	exptl	opt	exptl	opt
					(a) MSXX					
relative	0	0	0.76	0.78	0.22	0.30	0.70	0.69		0.46
total	−121.54	−121.67	−120.78	−120.89	−121.32	−121.37	−120.84	−120.98	–	−121.21
bond	0.18	0.18	0.19	0.18	0.17	0.18	0.19	0.18	–	0.19
angle	7.62	6.65	8.15	7.27	7.81	6.89	8.15	7.29	–	6.89
torsion	5.48	5.45	4.57	4.56	5.15	5.17	4.56	4.54	–	5.15
vdW	0.28	0.29	0.98	1.22	0.42	0.58	0.91	1.13	–	0.66
Q	−135.10	−135.25	−134.67	−135.06	−134.87	−135.17	−134.66	−135.07	–	−135.07
ZPE[b,d]		25.21		25.12		25.11		25.14		25.07
F (300 K)[c,d]		−2.41		−2.48		−2.41		−2.41		−2.48
relative (300 K)		0.0		0.62		0.20		0.62		0.25
					(b) MSXXS					
relative	0	0	0.72	0.72	0.39	0.46	0.72	0.67		0.64
total	−129.55	−129.72	−128.83	−129.00	−129.16	−129.26	−128.83	−129.05	–	−129.08
bond	0.37	0.36	0.35	0.39	0.35	0.38	0.36	0.39	–	0.38
angle	10.67	10.73	11.14	11.24	10.79	10.85	11.15	11.31	–	10.86
torsion	4.58	4.55	4.96	4.94	4.88	4.90	4.95	4.92	–	4.90
vdW	0.25	0.29	1.00	1.38	0.36	0.62	0.86	1.25	–	0.69
Q	−146.83	−146.94	−150.63	−151.68	−147.84	−148.43	−150.48	−151.66	–	−148.25
pol	1.41	1.30	4.36	4.73	2.31	2.42	4.32	4.76	–	2.35
Q + pol	−145.42	−145.64	−146.27	−146.95	−145.53	−146.01	−146.16	−146.90	–	−145.90
ZPE[b,e]		25.07		25.08		25.09		25.11		25.05
F (300 K)[c,e]		−2.47		−2.48		−2.41		−2.43		−2.49
relative (300 K)		0.0		0.72		0.54		0.75		0.60

[a] Energy components are also shown (the angle energy includes all cross terms, Q is the electrostatic energy, and pol is the polarization energy). [b] Zero-point energy. [c] Free energy at 300 K. [d] Calculated by using 10 × 10 × 10 points in the Brillouin zone. [e] Calculated by using 5 × 5 × 5 points in the Brillouin zone.

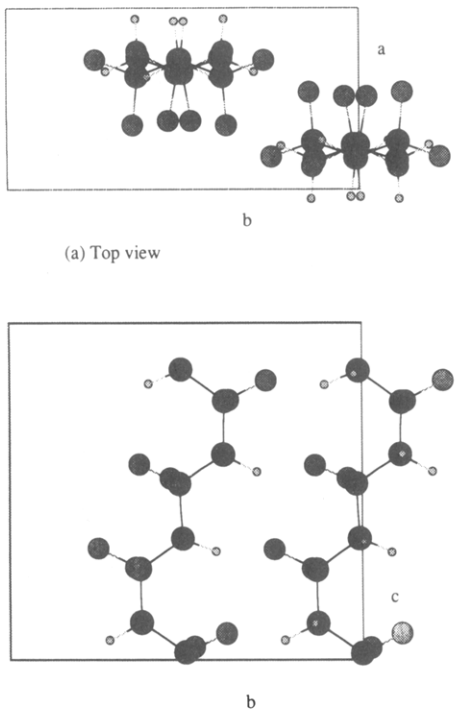

Figure 4. The end view (a) and the side view (b) of the antipolar form III crystal of PVDF.

ABCA/Ewald procedures.[21] In crystals with charged centers, the macroscopic field inside a crystal depends on the shape and surface states of the crystal. However, the Ewald method gives unique properties for any given cell parameters and coordinates of atoms. This is because the Ewald method assumes a perfect periodic system with no surface charges or surface dipoles so that the electric field and potential inside the crystal are periodic functions. Physically, the Ewald method gives the properties of the crystal for the case where the crystal is an infinitely large sphere immersed in a conducting medium.[22]

The elastic stiffness constants (C_{IJ}) and compliance constants (S_{IJ}) are defined as

$$\sigma_I = C_{IJ} e_J \tag{16}$$

$$e_J = S_{JI} \sigma_I \tag{17}$$

where e_J are components of strain and σ_I are components of stress (repeated indices are summed, Einstein convention). Here $I, J = 1, 2, ..., 6$ denotes xx, yy, zz, yz, zx, and xy, respectively.

The bulk modulus (β) is defined by

$$\beta^{-1} = \sum_{I,J=1}^{3} S_{IJ}$$

and Young's modulus in the chain direction is defined by

$$E_c = \sigma_c / e_c \tag{18}$$

where e_c and σ_c are strain and stress in the chain direction.

Table X shows the calculated values for all five forms.

On the basis of E_c, the strength of these crystal is in the sequence $I_p > II_{pd} > II_{ad} > III_{pu} > III_{au}$.

The MSXXS with its inclusion of shell polarization effects leads to a decrease in the elastic constants by about 10%. These changes arise from changes in the valence parameters for MSXXS.

The experimental Young modulus of the form I_p crystal in the chain direction quoted in ref 23 is 177 GPa. In this experiment, stress is applied along the chain direction and a shift of the characteristic X-ray diffraction spots associated with periodic structures in the polymer is observed. The elastic modulus is then calculated under the assumption of homogeneous stress. This value is much smaller than our calculated value of 283 GPa. We believe that the discrepancy is caused mainly by the difficulty in extracting the properties of a pure crystal from samples which have a mixture of the crystalline and amorphous regions. Similar results were found for polyethylene where the X-ray methods led to $E_c \approx 235$ GPa whereas neutron

Table X

(a) Elastic Stiffness Constants (GPa) of PVDF Calculated at the Experimental Structures (Except for Form III_{au}, Where the Optimized Structure Is Used)

MSXX						MSXXS					
					Form I_p						
25.5	3.0	4.0	0.0	0.0	0.0	23.7	2.4	4.7	0.0	0.0	0.0
3.0	12.4	2.4	0.0	0.0	0.0	2.4	11.8	3.1	0.0	0.0	0.0
4.0	2.4	283.4	0.0	0.0	0.0	4.7	3.1	266.8	0.0	0.0	0.0
0.0	0.0	0.0	3.5	0.0	0.0	0.0	0.0	0.0	3.7	0.0	0.0
0.0	0.0	0.0	0.0	5.1	0.0	0.0	0.0	0.0	0.0	5.2	0.0
0.0	0.0	0.0	0.0	0.0	4.0	0.0	0.0	0.0	0.0	0.0	4.0
					Form II_{ad}						
23.5	7.1	−5.5	0.0	−3.1	0.0	22.4	6.3	−7.4	0.0	−3.1	0.0
7.1	13.8	9.1	0.0	0.5	0.0	6.3	13.1	7.9	0.0	0.0	0.0
−5.5	9.1	162.8	0.0	0.4	0.0	−7.4	7.9	148.4	0.0	0.3	0.0
0.0	0.0	0.0	2.6	0.0	0.5	0.0	0.0	0.0	3.8	0.0	0.2
−3.1	0.5	0.4	0.0	6.8	0.0	−3.1	0.0	0.3	0.0	7.6	0.0
0.0	0.0	0.0	0.5	0.0	6.1	0.0	0.0	0.0	0.2	0.0	5.3
					Form III_{pu}						
19.9	7.3	−1.8	0.0	−0.8	0.0	19.2	6.3	−2.7	0.0	−0.6	0.0
7.3	15.0	10.6	0.0	−0.4	0.0	6.3	14.4	9.8	0.0	−0.6	0.0
−1.8	10.6	118.5	0.0	−0.9	0.0	−2.7	9.8	106.9	0.0	−1.0	0.0
0.0	0.0	0.0	2.7	0.0	−0.4	0.0	0.0	0.0	2.7	0.0	−0.4
−0.8	−0.4	−0.9	0.0	2.5	0.0	−0.6	−0.6	−1.0	0.0	2.8	0.0
0.0	0.0	0.0	−0.4	0.0	8.2	0.0	0.0	0.0	−0.4	0.0	7.7
					Form II_{pd}						
24.4	5.8	−4.7	0.0	0.0	0.0	22.7	4.6	−7.2	0.0	0.0	0.0
5.8	11.2	6.3	0.0	0.0	0.0	4.6	10.2	5.5	0.0	0.0	0.0
−4.7	6.3	162.6	0.0	0.0	0.0	−7.2	5.5	146.8	0.0	0.0	0.0
0.0	0.0	0.0	2.8	0.0	0.0	0.0	0.0	0.0	3.9	0.0	0.0
0.0	0.0	0.0	0.0	6.8	0.0	0.0	0.0	0.0	0.0	7.6	0.0
0.0	0.0	0.0	0.0	0.0	6.3	0.0	0.0	0.0	0.0	0.0	5.1
					Form III_{au}						
20.2	7.4	14.6	0.0	0.0	0.0	22.3	8.1	15.9	0.0	0.0	0.0
7.4	17.5	−1.8	0.0	0.0	0.0	8.1	19.0	−2.6	0.0	0.0	0.0
14.6	−1.8	115.9	0.0	0.0	0.0	15.9	−2.6	108.1	0.0	0.0	0.0
0.0	0.0	0.0	3.4	0.0	0.0	0.0	0.0	0.0	4.1	0.0	0.0
0.0	0.0	0.0	0.0	2.3	0.0	0.0	0.0	0.0	0.0	2.6	0.0
0.0	0.0	0.0	0.0	0.0	7.2	0.0	0.0	0.0	0.0	0.0	7.5

(b) Young's Modulus in the Chain Direction (E_c) and Bulk Modulus (β) for All Forms of PVDF (GPa)[a]

	form I_p		form II_{ad}		form III_{pu}		form II_{pd}		form III_{au}	
	exptl	opt	exptl	opt	exptl	opt	exptl	opt	exptl	opt
					MSXX					
E_c	282.5	292.7	151.2	152.9	107.7	113.4	156.0	162.8	–	101.7
β	9.5	14.8	11.7	12.4	11.7	13.3	9.8	12.1	–	12.5
					MSXXS					
E_c	265.2	277.2	136.8	140.9	97.2	107.2	139.3	150.2	–	92.3
β	8.8	15.2	10.5	13.6	10.8	14.7	8.6	13.6	–	13.5

[a] Calculations were carried out using the experimental cell parameters (exptl) and the optimized cell parameters (opt).

inelastic scattering, Raman, and theory all lead to 322 ± 9 GPa.

Including both strain and electric field as independent variables leads to the relations

$$\sigma_I = C_{IJ}e_J - g_{kI}\mathcal{E}_k \tag{19a}$$

$$\mathcal{P}_k = g_{kJ}e_J + a_{kl}\mathcal{E}_l \tag{19b}$$

where $\mathcal{E}$ is the external electric field and $\mathcal{P}$ is the dielectric polarization. Here **g** is the piezoelectric constant tensor[20] and **a** is the dielectric susceptibility tensor at constant strain. Alternatively, considering both stress and electric field as independent variables leads to

$$e_I = S_{IJ}\sigma_J + d_{kI}\mathcal{E}_k \tag{20a}$$

$$\mathcal{P}_k = d_{kJ}\sigma_J + b_{kl}\mathcal{E}_l \tag{20b}$$

where **d** is the piezoelectric modulus tensor and **b** is the dielectric susceptibility tensor at constant stress. These are related by[20]

$$d_{kI} = g_{kJ}S_{JI} \tag{21}$$

The **a** and **b** tensors are used to calculate the dielectric constant tensors at constant strain ($\epsilon^e = 1 + 4\pi\mathbf{a}$) and at constant stress ($\epsilon^\sigma = 1 + 4\pi\mathbf{b}$). The difference between the dielectric tensor at constant stress and that at constant strain is given by

$$\epsilon_{ij}^{\ \sigma} - \epsilon_{ij}^{\ e} = 4\pi\sum_K d_{iK}g_{jK} \tag{22}$$

It is well known that dielectric constants depend on frequency. At zero frequency, both the core and shell respond to an electric field. On the other hand, at infinite frequency, only the shell can respond to an electric field. Therefore, we calculate the dielectric constant at zero (ω

Table XI
Dielectric Constants of PVDF at Constant Strain (ϵ^e) at Zero Frequency ($\omega = 0$) and Infinite Frequency ($\omega = \infty$) and at Constant Stress (ϵ^σ) Calculated at the Experimental Structure (Except for Form III_{au}, Where the Optimized Structure Is Used)

(a) Constant Strain

MSXX ($\omega = 0$)			MSXXS ($\omega = 0$)			MSXXS ($\omega = \infty$)		
				Form I_p				
1.1210	0.0000	0.0000	2.1475	0.0000	0.0000	1.9113	0.0000	0.0000
0.0000	1.4480	0.0000	0.0000	2.7324	0.0000	0.0000	1.9050	0.0000
0.0000	0.0000	1.0687	0.0000	0.0000	1.9549	0.0000	0.0000	1.8557
				Form II_{ad}				
1.2242	0.0000	−0.0706	2.2338	0.0000	−0.1434	1.8987	0.0000	−0.0178
0.0000	1.1943	0.0000	0.0000	2.1385	0.0000	0.0000	1.8325	0.0000
−0.0706	0.0000	1.1377	−0.1434	0.0000	2.1603	−0.0178	0.0000	1.8678
				Form III_{pu}				
1.2521	0.0000	−0.0692	2.2892	0.0000	−0.1364	1.8798	0.0000	−0.0120
0.0000	1.1481	0.0000	0.0000	2.0994	0.0000	0.0000	1.8446	0.0000
−0.0692	0.0000	1.1455	−0.1364	0.0000	2.1653	−0.0120	0.0000	1.8839
				Form II_{pd}				
1.2159	0.0000	0.0000	2.2422	0.0000	0.0000	1.8972	0.0000	0.0000
0.0000	1.1733	0.0000	0.0000	2.1282	0.0000	0.0000	1.8320	0.0000
0.0000	0.0000	1.1372	0.0000	0.0000	2.1518	0.0000	0.0000	1.8668
				Form III_{au}				
1.1802	0.0000	0.0000	2.1302	0.0000	0.0000	1.8624	0.0000	0.0000
0.0000	1.2918	0.0000	0.0000	2.2968	0.0000	0.0000	1.9030	0.0000
0.0000	0.0000	1.1466	0.0000	0.0000	2.1833	0.0000	0.0000	1.9021

(b) Constant Stress

MSXX ($\omega = 0$)			MSXXS ($\omega = 0$)		
			Form I_p		
1.8012	0.0000	0.0000	2.8716	0.0000	0.0000
0.0000	1.4638	0.0000	0.0000	2.8599	0.0000
0.0000	0.0000	1.2848	0.0000	0.0000	2.4405
			Form II_{ad}		
1.2242	0.0000	−0.0706	2.2338	0.0000	−0.1434
0.0000	1.1943	0.0000	0.0000	2.1385	0.0000
−0.0706	0.0000	1.1377	−0.1434	0.0000	2.1603
			Form III_{pu}		
1.3343	0.0000	−0.1284	2.4571	0.0000	−0.1860
0.0000	1.1839	0.0000	0.0000	2.1608	0.0000
−0.1284	0.0000	1.4326	−0.1860	0.0000	2.4544
			Form II_{pd}		
1.2597	0.0000	0.0000	2.3340	0.0000	0.0000
0.0000	1.2105	0.0000	0.0000	2.1501	0.0000
0.0000	0.0000	1.2127	0.0000	0.0000	2.2228
			Form III_{au}		
1.1802	0.0000	0.0000	2.1545	0.0000	0.0000
0.0000	1.2948	0.0000	0.0000	2.3010	0.0000
0.0000	0.0000	1.2115	0.0000	0.0000	2.2507

= 0) and infinite ($\omega = \infty$) frequencies as follows:

$$\epsilon_{ij}^{e}(\omega=0) = \delta_{ij} + C_{\text{unit}}(4\pi/\Omega)\sum_{m,n} q_m q_n D_{mi,nj}^{\text{all}} \quad (23a)$$

$$\epsilon_{ij}^{e}(\omega=\infty) = \delta_{ij} + C_{\text{unit}}(4\pi/\Omega)\sum_{m,n} Z_m Z_n D_{mi,nj}^{\text{shell}} \quad (23b)$$

Here, D^{all} is the inverse of Hessian of all centers and the sum is over all centers (see (13)). D^{shell} is the inverse of Hessian of shells at fixed core positions and the sum is over shells. q_m is the charge of a center m, and Ω is the volume of the cell. For the MSXX force field, $\epsilon_{ij}^{e}(\omega=\infty) = \delta_{ij}$.

Table XI shows ϵ^e and ϵ^σ for all the forms and both force fields at zero and infinite frequencies. For form I, the axes are transformed such that the orientation is the same one used in the experiments (axis 1 is parallel to chain direction c, axis 2 is parallel to a, and axis 3 is parallel to b and the polarization direction). As expected MSXXS has a dramatic effect. The experimental determination of the properties for the crystalline form is quite difficult since the dielectric constant of the amorphous region is quite large and depends strongly on temperature and frequency. Measurements using the oriented films of the form I crystal[24] give $\epsilon_3 = 3.6$ (−106 °C, 0.065 MHz), 3.7 (−100 °C, 0.049 MHz), and 3.1 (−102 °C, 0.059 MHz) which should be compared with the calculated value of $\epsilon_3^\sigma(\omega=0) = 2.44$ for MSXXS ($\epsilon_3^e(\omega=0) = 1.95$). The calculated value is smaller than experiment, but this may be due to the amorphous regions in the experimental sample.

Table XII shows the piezoelectric moduli (**d**) at the experimental cell parameters for all forms (piezoelectric constants (**g**) can be calculated by using (21)). In form I_p, the axes are transformed as in the dielectric constants for comparison with the experiment. In form II_{pd}, the a and c axes are interchanged such that these values are compared directly with form I_p (axis 1 is parallel to the chain direction c, axis 2 is parallel to a, and axis 3 is parallel to b, the polarization direction). In form II_{ad}, the calculated values of these constants are zero as expected by space group symmetry (not shown in the table). Comparing calculated values between MSXX and MSXXS shows that piezoelectric constants generally increase for MSXXS (by

Table XII
Piezoelectric Modulus Tensor d_{ij} (pC/N) Where J = 1–6 and i = 1–3[a]

MSXX						MSXXS					
					Form I_p						
0.0	0.0	0.0	0.0	−41.3	0.0	0.0	0.0	0.0	0.0	−41.9	0.0
0.0	0.0	0.0	−5.9	0.0	0.0	0.0	0.0	0.0	−16.8	0.0	0.0
0.07	1.1	−12.7[b]	0.0	0.0	0.0	0.57	−1.3	−18.8[b]	0.0	0.0	0.0
					Form III_{pu}						
0.80	4.9	−2.0	0.0	−1.3	0.0	4.4	4.2	−2.7	0.0	−1.2	0.0
0.0	0.0	0.0	3.7	0.0	6.1	0.0	0.0	0.0	12.0	0.0	5.1
3.5	−3.5	2.1	0.0	29.1	0.0	3.3	−1.6	2.2	0.0	27.6	0.0
					Form II_{pd}						
0.0	0.0	0.0	0.0	−9.9	0.0	0.0	0.0	0.0	0.0	−9.1	0.0
0.0	0.0	0.0	−7.3	0.0	0.0	0.0	0.0	0.0	−6.1	0.0	0.0
1.4	−3.5	0.15	0.0	0.0	0.0	1.8	−2.4	−2.9	0.0	0.0	0.0
					Form III_{au}						
0.0	0.0	0.0	0.0	−0.08	0.0	0.0	0.0	0.0	0.0	9.1	0.0
0.0	0.0	0.0	2.8	0.0	0.0	0.0	0.0	0.0	3.0	0.0	0.0
−4.0	3.3	2.1	0.0	0.0	0.0	−3.5	4.0	2.2	0.0	0.0	0.0
					Form II_{au}						
0.0	0.0	0.0	0.0	1.6	0.0	0.0	0.0	0.0	0.0	1.15	0.0
0.0	0.0	0.0	3.3	0.0	0.0	0.0	0.0	0.0	3.85	0.0	0.0
2.5	−3.0	0.79	0.0	0.0	0.0	3.28	−2.54	0.71	0.0	0.0	0.0

[a] Calculations are at the experimental structures (except for form III_{au}, where the optimized structure is used). [b] Experimental value (ref 23) is −20 ± 5.

30% for form I), but the effect is smaller than for dielectric constants.

The experimental value[23] of d_{33} of the form I_p crystal is −20 ± 5 pC/N, which is quite close to the calculated value with the shell model of −18.8 pC/N. Also, the experimental value of d_{31} is reported to be much smaller than d_{33}, which is consistent with our results, d_{31}/d_{33} = −0.5/18.8 = −0.02.

Although the Lovinger form (III_{au}) has no net polarization in the direction perpendicular to the chain, the piezoelectric moduli are nonzero as shown in Table XII (the space-group symmetry allows nonzero values). The calculated values are similar to those of form III_{pu} except that III_{pu} has a small value for the shear piezoelectric modulus.

VII. Calculations with Both Chain Alignments

For forms II_{ad}, III_{pu}, and III_{au}, the dipoles along two chains in the unit cell can be aligned in the same direction (up–up) or in the opposite direction (up–down). Using the MSXX force field, we optimized the structure for both chain alignments; see Table VIII. After optimization, the elastic constants were calculated for each structure where we found that each structure is mechanically stable.

For the II_{ad} crystal, the optimized cell of the up–up structure is orthorhombic, and the energy is almost the same as that of the up–down structure. The difference between optimized cell parameters of the up–down structure and the up–up structure is small except for an angle β. This supports the interpretation of X-ray results that, in the II_a crystal, up chains and down chains are packed statistically.[16] Also, it suggests that the II_a crystal with up–up packing could be formed experimentally. In fact, Newman and Scheinbeim[25] suggested this structure from the sample obtained by poling unoriented form II_a films. Since there is a net dipole moment in the chain direction in the up–up structure, piezoelectric moduli are nonzero in this crystal. These constants were calculated at the experimental cell parameters by using both MSXX and MSXXS (see Table XII).

For the III_{pu} crystal, the energy of the up–down structure (III_{pd}) is 1.6 kcal/mol higher than that of the up–up structure (III_{pu}). This agreement with experiment,[17] which finds the up–up structure (with some disorder).

For the form II_{pd} crystal, the energy of the up–up structure is calculated to be within 0.01 kcal/mol of the up–down structure, but the optimized unit cell of the up–up structure is monoclinic and the β cell angle is 104° (which corresponds to a relative shift of the two chains in the chain direction). Considering the small energy difference between these two structures, it seems to be reasonable to assume the statistical packing of up and down chains in the unit cell in this form, as suggested by Bachmann et al.[18]

For the form III_{au} crystal, the optimized up–down unit cell is monoclinic with β = 120°, and the energy is about 0.7 kcal/mol higher than that of the up–up structure. Since the up–down crystal has inversion symmetry, all piezoelectric constants vanish for this structure.

VIII. Comparison with Other Calculations

Tashiro et al.[23] (TKTF) calculated the elastic and the piezoelectric constants of a form I_p crystal using a point-charge model. In the TKTF calculations, the valence parameters and nonbonding parameters were determined by fitting to the experimental vibrational frequencies. The main differences between this study and TKTF are the following: (1) In TKTF the long-range Coulomb interactions are ignored, whereas we include them (using the ABCA/Ewald method[21]). (2) In TKTF, the atomic polarizabilities are not considered, whereas we include them using MSXXS. (3) We considered nine crystalline forms (including five new ones) instead of just I_p.

The elastic-stiffness constants of both calculations are quite similar except that C_{33} is about 10% smaller in TKTF. For the piezoelectric modulus tensor, the discrepancies are noticeable. For d_{33} we obtain −18.8 pC/N while TKTF obtain −25.2 and experiment gives −20. Also the sign of d_{31} is different. For d_{24} we obtain −16.8 while TKTF obtain −4.28, and a recent measurement of the shear piezoelectric constants[26] gives a d_{24} of −38.3 pC/N. From comparing the results between TKTF and MSXX, it appears that the long-range Coulomb interactions do not have a large effect on these properties.

IX. Comparison with Processing Results

In Figure 5 we sketch the relationships between various forms and processing conditions (mainly adapted from

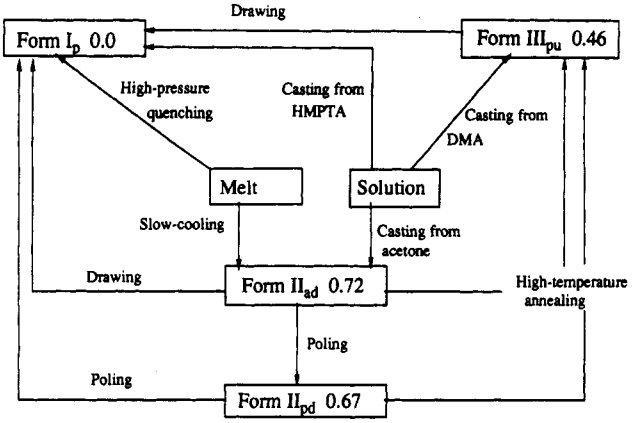

Figure 5. Processing relationships between forms. The calculated energies per CH_2CF_2 using the MSXXS force field are shown. HMPTA = hexamethylphosphorictriamide; DMA = dimethylacetamide.

ref 23b, but also from refs 27–35). Included in the sketch are our calculated energies. We see here that the energetics are quite consistent with observed processing. Thus, cooling from the melt leads to II_a (E = 0.72 kcal/mol). Drawing at room temperature leads to I_p (E = 0.0). Poling (application of external electric fields) leads to the polar form II_p (with E = 0.67). High-temperature annealing from II_p leads to III_p (E = 0.46). Poling from II_p or drawing from III_p leads to I_p.

X. Summary

A force field including the covalent shell model was developed and applied to nine crystal forms of PVDF crystals (four of which are observed experimentally). Structural, elastic, dielectric, and piezoelectric properties were calculated for all the crystal forms. We find five stable structures not yet observed experimentally, each of which is mechanically stable with energy comparable to the other forms.

Acknowledgment. We thank Jean-Marc Langlois and Dr. Murco N. Ringnalda (Schrödinger, Inc.) for carrying out the PS-Q calculations for charges. We also thank Dr. Siddharth Dasgupta for helpful discussions about fitting force fields and torsional potentials. This research was partially funded by Allied-Signal, BP America, Asahi Chemical, Asahi Glass, and Chevron Inc. These studies used the FPS 522, Alliant FX80/8, and Silicon Graphics 380/8 computers of the MSC/BI which were funded by grants from DOE/AICD, DARPA/ONR, NSF-DMR, and NSF-CHE.

Supplementary Material Available: Tables of fractional coordinates of the Lovinger structure III_{au}, piezoelectric constants of the four forms, and elastic constants and piezoelectric moduli of form I (3 pages). Ordering information is given on any current masthead page.

References and Notes

(1) Lovinger, A. J. *Macromolecules* **1981**, *14*, 322.
(2) Karasawa, N.; Dasgupta, S.; Goddard, W. A., III. *J. Phys. Chem.* **1991**, *95*, 2260.
(3) Tashiro, K.; Itoh, Y.; Kobayashi, M.; Tadokoro, H. *Macromolecules* **1985**, *18*, 2600.
(4) These calculations were carried out using (a) Gaussian 88: Frisch, M. J.; Head-Gordon, M.; Schlegel, H. B.; Raghavachari, K.; Binkley, J. S.; Gonzalez, C.; Defrees, D. J.; Fox, D. J.; Whiteside, R. A.; Seeger, R.; Melius, C. F.; Baker, J.; Martin, R. L.; Kahn, L. R.; Stewart, J. J. P.; Fluder, E. M.; Topiol, S.; Pople, J. A., Gaussian, Inc., Pittsburgh, PA, 1988. (b) Gaussian 90: Frisch, M. J.; Head-Gordon, M.; Trucks, G. W.; Foresman, J. B.; Schlegel, H. B.; Raghavachari, K.; Robb, M. A.; Binkley, J. S.; Gonzalez, C.; Defrees, D. J.; Fox, D. J.; Whiteside, R. A.; Seeger, R.; Melius, C. F.; Baker, J.; Martin, R. L.; Kahn, L. R.; Stewart, J. J. P.; Topiol, S.; Pople, J. A., Gaussian, Inc., Pittsburgh, PA, 1990.
(5) (a) Woods, R. J.; Khalil, M.; Pell, W.; Moffat, S. H.; Smith, V. H., Jr. *J. Comput. Chem.* **1990**, *11*, 297. (b) Our calculations of electrostatic potential derived charges were carried out using the PS-Q program [Langlois, J-M.; Ringnalda, M. N.; Goddard, W. A., III; Friesner, R. Unpublished results] based on the pseudospectral Hartree–Fock method. See: Ringnalda, M. N.; Won, Y.; Friesner, R. A. *J. Chem. Phys.* **1990**, *92*, 1163 and references therein for the PS program.
(6) Rappé, A. K.; Goddard, W. A., III. *J. Phys. Chem.* **1991**, *95*, 3358.
(7) Goddard, W. A., III.; Karasawa, N. Elastic Constants and Phonon States for Graphite; van der Waals Parameters for Carbon. *J. Phys. Chem.*, submitted for publication.
(8) Maekawa, T.; Karasawa, N.; Goddard, W. A., III. To be published.
(9) (a) The force field parameter optimization was carried out using the FFOPT program: Yamasaki, T.; Dasgupta, S.; Goddard, W. A., III. To be published. (b) Dasgupta, S.; Goddard, W. A., III. *J. Chem. Phys.* **1989**, *90*, 7207.
(10) (a) Dick, B. G., Jr.; Overhauser, A. W. *Phys. Rev.* **1958**, *112*, 90. (b) Brüesch, P. *Phonons: Theory and Experiments I*; Springer-Verlag: Berlin, 1982.
(11) The Biograf/Polygraf program[19] from Molecular Simulations Inc. was modified to automatically include these modifications for the covalent shell model.
(12) Karasawa, N.; Goddard, W. A., III. *Covalent Shell Model and Polarizabilities of Fluoroalkanes*; to be published.
(13) Applequist, J. *Acc. Chem. Res.* **1977**, *10*, 79.
(14) Boyd, R. H.; Kesner, L. *J. Chem. Phys.* **1980**, *72*, 2179.
(15) Hasegawa, R.; Takahashi, Y.; Chatani, Y.; Tadokoro, H. *Polym. J.* **1972**, *3*, 600.
(16) Takahashi, Y.; Matsubara, Y.; Tadokoro, H. *Macromolecules* **1983**, *16*, 1588.
(17) Takahashi, Y.; Tadokoro, H. *Macromolecules* **1980**, *13*, 1317.
(18) Bachmann, M.; Gordon, W. L.; Weinhold, S.; Lando, J. B. *J. Appl. Phys.* **1980**, *51*, 5095.
(19) The molecular dynamics calculations and geometry/cell optimization were carried out using POLYGRAF, an interactive molecular simulation/three-dimensional graphics program from Molecular Simulations Inc., Waltham, MA.
(20) Born, M.; Huang, K. *Dynamical Theory of Crystal Lattices*; Oxford University Press: Oxford, 1954.
(21) Karasawa, N.; Goddard, W. A., III. *J. Phys. Chem.* **1989**, *93*, 7320.
(22) De Leeuw, S. W.; Perram, J. W.; Smith, E. R. *Proc. R. Soc. London* **1980**, *A373*, 27.
(23) (a) Tashiro, K.; Kobayashi, M.; Tadokoro, H.; Fukada, E. *Macromolecules* **1980**, *13*, 691. (b) Tashiro, K.; Tadokoro, H.; Kobayashi, M. *Ferroelectrics* **1981**, *32*, 167.
(24) Ohigashi, H. *J. Appl. Phys.* **1976**, *47*, 949.
(25) Newman, B. A.; Scheinbeim, J. I. *Macromolecules* **1983**, *16*, 60.
(26) Nix, E. L.; Ward, I. M. *Ferroelectrics* **1986**, *67*, 137.
(27) Lando, J. B.; Olf, H. G.; Peterlin, A. *J. Polym. Sci., Part A-1* **1966**, *4*, 941.
(28) Doll, W. W.; Lando, J. B. *J. Macromol. Sci.* **1970**, *B4*, 309.
(29) Davis, G. T.; McKinney, J. E.; Broadhurst, M. G.; Roth, S. C. *J. Appl. Phys.* **1978**, *49*, 4998.
(30) Dasgupta, D. K.; Doughty, K. *J. Appl. Phys.* **1978**, *49*, 4601.
(31) Scheinbeim, J.; Nakafuku, C.; Newman, B. A.; Pac, K. D. *J. Appl. Phys.* **1979**, *50*, 4399.
(32) Osaki, S.; Ishida, Y. *J. Polym. Sci., Polym. Phys. Ed.* **1975**, *13*, 1071.
(33) Prest, W. M., Jr.; Luca, D. J. *J. Appl. Phys.* **1975**, *46*, 4136.
(34) Servet, B.; Rault, J. *J. Phys.* **1979**, *40*, 1145.
(35) Kobayashi, M.; Tashiro, K.; Tadokoro, H. *Macromolecules* **1975**, *8*, 158.
(36) Tashiro, K.; Kobayashi, M.; Tadokoro, H. *Macromolecules* **1981**, *14*, 1757.
(37) Durig, J. R.; Guirgis, G. A.; Li, Y. S. *J. Chem. Phys.* **1981**, *74*, 5946.

Registry No. PVDF, 24937-79-9.